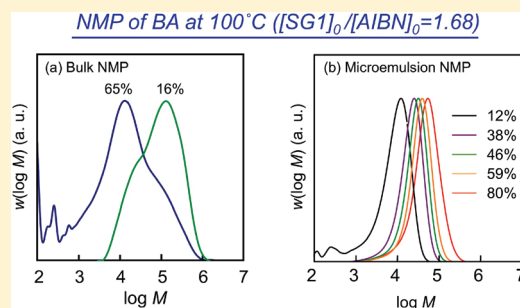


Nitroxide-Mediated Radical Polymerization in Microemulsion (Microemulsion NMP) of *n*-Butyl Acrylate<sup>†</sup>Seita Tomoeda, Yukiya Kitayama, Junpei Wakamatsu, Hideto Minami, Per B. Zetterlund,<sup>‡</sup> and Masayoshi Okubo\*

Graduate School of Engineering, Kobe University, Kobe 657-8501, Japan

**ABSTRACT:** Nitroxide-mediated radical polymerization (NMP) in microemulsion (microemulsion NMP) of *n*-butyl acrylate (BA) has been carried out at 100 °C using *N*-tert-butyl-*N*-(1-diethylphosphono-2,2-dimethylpropyl) nitroxide (SG1), 2,2'-azoisobutyronitrile (AIBN), and the cationic emulsifier tetradecyltrimethylammonium bromide (TTAB). At [SG1]<sub>0</sub>/[AIBN]<sub>0</sub> of 1.68 (molar ratio), the polymerization exhibited classical trend marks of a controlled/living system with the molecular weight distribution (MWD) shifting to higher molecular weights with increasing conversion and a linear increase in number-average molecular weight ( $M_n$ ) vs conversion. Bulk NMP carried out under the same conditions (without water and TTAB) proceeded at an extremely high rate without control/livingness. From these results, it is concluded that the confined space effect (compartmentalization) operates in the microemulsion NMP; in other words, it is a useful tool to prepare nanosized monomer-solubilized micelles for regulation and improvement of NMP.



## INTRODUCTION

Controlled/living radical polymerization (CLRP) has been studied extensively over the past 15 years, and it is now possible to prepare well-defined polymers with controlled molecular weight, narrow molecular weight distribution, and complex architecture (such as block, graft, and star polymers) by free radical means.<sup>1</sup> A variety of CLRP techniques have been developed, most notably nitroxide-mediated radical polymerization (NMP),<sup>2,3</sup> atom transfer radical polymerization (ATRP),<sup>4,5</sup> and reversible addition–fragmentation chain transfer (RAFT) polymerization.<sup>6</sup> These CLRP methods have been investigated mainly in homogeneous systems (bulk and solution polymerizations). In recent years, much effort has been directed to apply to CLRP to aqueous dispersed systems (suspension, emulsion, miniemulsion and microemulsion polymerizations)<sup>7,8</sup> due to environmental concerns and industrialization. Moreover, we are interested in the preparation of novel types of functional particles using CLRP in an aqueous dispersed systems.<sup>9–12</sup>

In a series of theoretical investigations on NMP and ATRP in dispersed systems, we and others have reported that compartmentalization can significantly influence the polymerization kinetics.<sup>13–27</sup> The concept of compartmentalization comprises two effects: the segregation effect and the confined space effect. In dispersed systems, propagating radicals are segregated between different particles/droplets, and consequently the termination rate decreases if the system is sufficiently segregated (the segregation effect). The rate of deactivation is enhanced by the confined space effect, which states that two species react at a higher rate in a small droplet/particle than in a large droplet/particle, under conditions where the overall deactivator (nitroxide in NMP, Cu(II) complex in ATRP) concentration in the dispersed phase is lower than that

in the specific droplet/particle where deactivation can occur. The segregation effect leads to an increase in polymerization rate ( $R_p$ ) and livingness (end-functionality) but less control (broader molecular weight distribution (MWD)). The confined space effect on deactivation leads to a reduction in  $R_p$  and improved control due to an increase in the number of activation–deactivation cycles experienced by a given polymer chain as it grows to a given degree of polymerization. The confined space effect may also increase the rate of geminate termination between the pair of radicals generated by spontaneous initiation of styrene as well as by organic phase initiators generating radicals in pairs. In addition, compartmentalized systems may also be influenced by the so-called fluctuation effect,<sup>17,27</sup> which refers to an overall decrease in the deactivation rate due to the fluctuation in the number of deactivator species between different particles. As part of our previous theoretical work on the confined space effect in NMP and ATRP, we have reported that in the case of NMP of styrene using 2,2,6,6-tetramethylpiperidyl-1-oxy (TEMPO) at 125 °C, the confined space effect is operative for droplet/particle diameters smaller than 65 nm for an initial alkoxyamine concentration of 0.02 M.<sup>15</sup>

Microemulsion polymerization is the dispersed phase polymerization system that gives access to the smallest particles, often as small as 10–20 nm diameters.<sup>28–30</sup> A general microemulsion polymerization system, which is composed of monomer, water, a large amount of surfactant (and sometimes a cosurfactant), is thermodynamically stable and consequently forms a stable emulsion spontaneously without external shear forces. Microemulsion

Received: April 14, 2011

Revised: June 7, 2011

Published: June 23, 2011

polymerization has recently been applied to RAFT,<sup>31–33</sup> ATRP,<sup>34–36</sup> and NMP.<sup>37,38</sup> In microemulsion RAFT, the segregation effect is operative on propagation radicals due to the particle diameter being sufficiently small. However, the confined space effect plays no role in RAFT polymerization under normal conditions because the RAFT end group concentration is too high.<sup>7,18</sup> Matyjaszewski and co-workers successfully conducted microemulsion ATRP,<sup>34,35</sup> but the corresponding bulk polymerizations were not investigated thus making it difficult to draw conclusions regarding compartmentalization effects. We also carried out microemulsion ATRP,<sup>39</sup> but were unable to compare the experimental data with theory due to exit of the control agent ( $\text{Cu}^{\text{II}}$ ). Microemulsion NMPs of styrene using tetradecyltrimethylammonium bromide (TTAB) as cationic surfactant and the three different nitroxides TEMPO, *N*-tert-butyl-*N*-(1-diethylphosphono-(2,2-dimethylpropyl)) nitroxide (SG1), and 2,2,5-trimethyl-4-phenyl-3-azahexane-3-oxy (TIPNO) at 125 °C were also reported.<sup>37,38</sup>  $R_p$  was lower in microemulsion than in bulk for all three nitroxides, and  $M_w/M_n$  was lower than in bulk for SG1 and TIPNO. Cunningham and co-workers reported that in the case of miniemulsion NMP of styrene using TEMPO,  $R_p$  decreased and the livingness increased with decreasing particle size.<sup>40</sup>

NMP of *n*-butyl acrylate (BA) is in general difficult due to the high propagation rate coefficient of BA.<sup>41</sup> This problem can be overcome by use of strongly hindered nitroxides with high NMP equilibrium constants,<sup>42–44</sup> or alternatively, satisfactory results in terms of control/livingness can be achieved by use of an initial excess of free nitroxide.<sup>45–50</sup> In the present contribution, microemulsion NMP of BA has been carried out at 100 °C using TTAB and SG1/2,2-azobis(isobutyronitrile) (AIBN) with a view to reducing the required amount of excess SG1 by exploitation of the confined space effect on deactivation.

## EXPERIMENTAL SECTION

**Materials.** BA was purified by distillation under reduced pressure in a nitrogen atmosphere. 2,2'-Azobisisobutyronitrile (AIBN; Wako Pure Chemicals, Japan) was purified by recrystallization. SG1 provided by ARKEMA K. K. (Japan) and *n*-tetradecyltrimethylammonium bromide (TTAB; Tokyo Kasei Kogyo Co. Ltd., Tokyo, Japan) was used as received. Deionized water with a specific resistance of 18.2 M  $\Omega$  cm was obtained an Elix UV (Millipore Japan) purification system.

**Microemulsion Polymerizations.** Typical procedure of microemulsion polymerization: a solution of SG1 (61 mg, 0.207 mmol), AIBN (20 mg, 0.122 mmol), and BA (6 g, 46.9 mmol) was added to an aqueous solution of TTAB (15 g, in 99 g water). After being stirred for 30 min with a magnetic stirrer at room temperature, the mixture became transparent (microemulsion). Approximately 20 mL of the microemulsion was charged in glass ampules and degassed using  $\text{N}_2$ /vacuum cycles, after which the ampules were sealed off. Microemulsion polymerization was conducted at 100 °C. The glass ampules were rapidly cooled in cool water at appropriate time interval, and conversion was measured by gas chromatography (GC-18A, Shimadzu Co., Kyoto, Japan) with helium as carrier gas, using *N,N*-dimethylformamide (DMF) and toluene as solvent and internal standard, respectively.

**Bulk Polymerizations.** Bulk polymerization of BA (6 g, 46.9 mmol) with SG1 (61 mg, 0.207 mmol) and AIBN (20 mg, 0.122 mmol) was conducted at 100 °C in the glass ampules after degassing using  $\text{N}_2$ /vacuum cycles. The conversion was measured in the same way as the microemulsion polymerization.

**Measurements.** Number- and weight-average molecular weights ( $M_n$  and  $M_w$ , respectively) and molecular weight distribution (MWD)

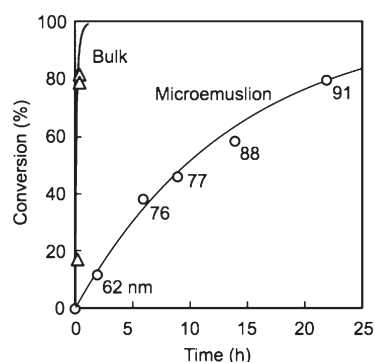


**Figure 1.** Conversion–time plots for (triangles) bulk and (circles) microemulsion NMPs of BA using SG1 at 100 °C:  $[\text{AIBN}]_0 = 18.6$  mmol/L-monomer;  $[\text{SG1}]_0/[\text{AIBN}]_0 = 1.68$ , molar ratio. The lines are guides to the eye only. The numbers are particle diameter (nm).

were analyzed by gel permeation chromatography (GPC) using two styrene/divinylbenzene gel columns [TOSHO Corporation, TSKgel GMH<sub>HR</sub>-H, 7.8 mm i.d.  $\times$  30 cm] using THF as eluent at 40 °C at a flow rate of 1.0 mL  $\cdot$  min<sup>−1</sup> with refractive index detection (TOSOH RI-8020/21). The columns were calibrated with PS standards ( $1.05 \times 10^3$  to  $5.48 \times 10^6$  g/mol). Particle size distributions were measured by dynamic light scattering (DLS-7000, Otsuka Electronics, Osaka Japan) at the light scattering angle of 90° at 25 °C after dilution with deionized water. Number- and weight-average particle diameters ( $D_n$  and  $D_w$ , respectively) were obtained using the Marquadt analysis routine.

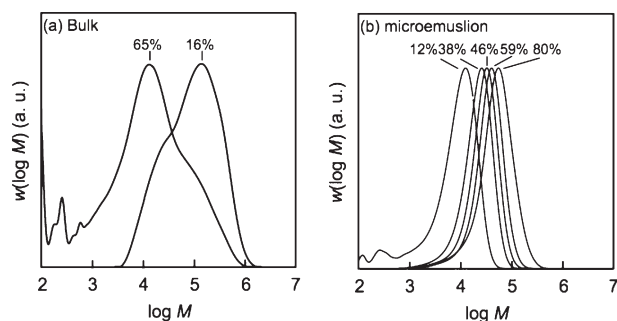
## RESULTS AND DISCUSSION

It has been reported that bulk NMP of BA using SG1/AIBN gives satisfactory control/livingness if a suitable excess amount of free nitroxide is added ( $[\text{SG1}]_0/[\text{AIBN}]_0$  molar ratios of 2–5).<sup>47,48</sup> Bulk and microemulsion NMPs of BA were conducted at  $[\text{SG1}]_0/[\text{AIBN}]_0 = 1.68$  at 100 °C with the expectation that control/livingness would not be obtained in the bulk system due to insufficient excess of SG1.

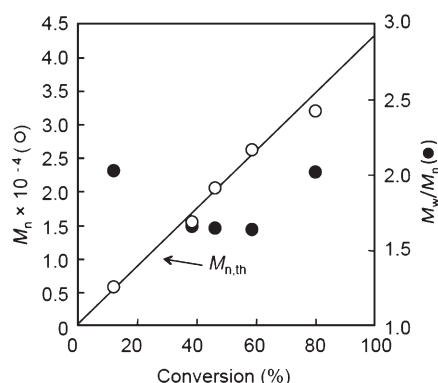
Figure 1 shows conversion–time plots for the bulk and microemulsion NMPs of BA. In the bulk NMP,  $R_p$  was very high with the conversion reaching as high as 80% in 10 min. The corresponding microemulsion system, on the other hand, was much slower, reaching 80% conversion in 22 h. Before polymerization, the microemulsion was transparent and the micelle size was about 1 to 2 nm. As the polymerization proceeded, the appearance changed to translucent or turbid and the  $D_n$  values above 12% conversion were fairly large (62 to 91 nm; discussed later).

Figure 2 shows MWDs for the bulk and microemulsion NMPs of BA. In the bulk NMP, MWD was very broad, with  $M_w/M_n$  was 21.0 at 65% conversion, clearly revealing that the polymerization proceeded without control. On the other hand, in the microemulsion NMP, the MWD shifted to higher molecular weight side with increasing conversion, indicating controlled/living character.

Figure 3 shows  $M_n$  and  $M_w/M_n$  as a function of the conversion for the microemulsion NMP. The theoretical  $M_n$  ( $M_{n,\text{th}}$ ) was calculated from the ratio of consumed monomer to radical generated from;  $M_{n,\text{th}} = ([\text{BA}]_0 \alpha M_{\text{BA}})/2f[\text{AIBN}]$ , where  $\alpha$  is BA conversion,  $M_{\text{BA}}$  is the molar mass of BA, and  $2f[\text{AIBN}]$  is the total concentration of radicals generated by AIBN ( $f$  is the initiator efficiency). In this case,  $f$  was set at 0.57.<sup>48,51</sup>  $M_n$  fitted  $M_{n,\text{th}}$  very well and  $M_w/M_n$  was relatively low ( $M_w/M_n = 1.6–2.0$ ) indicating well-controlled polymerization. On the basis



**Figure 2.** Molecular weight distributions (MWDs) at various conversions for (a) bulk (conversions: 16, 65%) and (b) microemulsion (conversions: 12, 38, 46, 59, 80%) NMPs of BA using SG1 at 100 °C:  $[AIBN]_0 = 18.6$  mmol/L-monomer;  $[SG1]_0/[AIBN]_0 = 1.68$ , molar ratio.



**Figure 3.**  $M_n$  and  $M_w/M_n$  vs conversion plots for microemulsion NMP of BA using SG1 at 100 °C:  $[AIBN]_0 = 18.6$  mmol/L-monomer;  $[SG1]_0/[AIBN]_0 = 1.68$ , molar ratio. The straight line is the  $M_{n,th}$ .

of the above data, it is apparent that the polymerization proceeds very differently in microemulsion compared to bulk, consistent with the confined space effect being operative.

In order to further study how the confined space effect can be exploited to improve the level of control/livingness in microemulsion NMP (Figure 4), additional polymerizations were carried out in both bulk and microemulsion at  $[SG1]_0/[AIBN]_0 = 1.60, 1.76$ , and  $1.92$  at constant  $[AIBN]_0$ . In all cases, the bulk NMPs proceeded without control/livingness; the  $R_p$  values were very high and the MWDs were broad, similar to when  $[SG1]_0/[AIBN]_0 = 1.68$  (Figures 1 and 2). In the microemulsion NMPs,  $R_p$  decreased with the slight increases in  $[SG1]_0/[AIBN]_0$ , the conversions reaching 80% in 22 h, 62% in 28 h and 60% in 36 h at  $[SG1]_0/[AIBN]_0$  ratios of 1.68, 1.76, and 1.92, respectively.

Parts a and b of Figure 5 show, respectively,  $D_n$ - and  $D_w$ -conversion plots at the various  $[SG1]_0/[AIBN]_0$  ratios. In all cases,  $D_n$  and  $D_w$  increased markedly in the initial stage of the polymerization (conversion <10%), and subsequently increased moderately during the remainder of the polymerization. At final conversions, the particle size distributions were narrow in all  $[SG1]_0/[AIBN]_0$  ratios (see Figure 6). At the  $[SG1]_0/[AIBN]_0$  ratio of 1.60 (which gave the highest  $R_p$ ), the measured  $D_n$  values were in 20–26 nm and the system remained transparent throughout the polymerization. At the  $[SG1]_0/[AIBN]_0$  ratios of 1.68, 1.76, and 1.92, the microemulsion systems became translucent or turbid, with the  $D_n$  values of 91, 133, and 184 nm, respectively, at approximately 60% conversion. Thus,

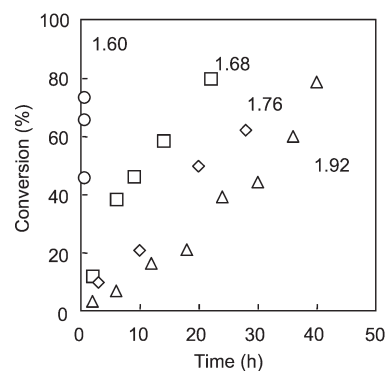


**Figure 4.** Conversion–time plots for microemulsion NMPs of BA using SG1 at 100 °C:  $[AIBN]_0 = 18.6$  mmol/L-monomer;  $[SG1]_0/[AIBN]_0$  (molar ratio) = 1.60 (circles); 1.68 (squares); 1.76 (diamonds); 1.92 (triangles).

there was a clear trend of the particle size increasing with increasing SG1 concentration (i.e., decreasing  $R_p$ ). The initial number of micelles is very large, and only a fraction of these micelles becomes nucleated and turns into polymer particles. In fact, some of the initial micelles may not contain any initiator/nitroxide. Monomer will diffuse from non-nucleated micelles (all micelles are swollen with monomer) to nucleated micelles (polymer particles), thus accounting for the increase in particle size with conversion. The extent of swelling of nucleated micelles is further increased when the polymerization proceeds by a controlled/living mechanism (i.e., NMP) due to the phenomenon known as superswelling.<sup>52</sup> The large number of oligomers formed in NMP at low conversion act as effective swelling agents; the swelling ability of oligomers is much higher than that of high molecular weight polymer.<sup>53,54</sup> In addition, the lower  $R_p$  at high  $[SG1]_0/[AIBN]_0$  allows more time for monomer diffusion to occur between non-nucleated micelles and polymer particles.

Figure 5c shows the number of polymer particles ( $N_p$ ) at several conversions at the various  $[SG1]_0/[AIBN]_0$  ratios. In all cases, the numbers of polymer particles immediately increased at the initial stage of the polymerizations, and then the values were maintained similarly, indicating that the number of polymer particles were fixed in the initial stage of the polymerizations. The increasing of  $[SG1]_0/[AIBN]_0$  ratio increases the deactivation rate, resulting in delay in the propagation of polymer chains, therefore, the larger number of oligomer chains, of which degree of polymerization (DP) does not attain the critical DP ( $DP_{cr}$ ) inhibiting the escape to the aqueous medium, seems to be formed in the initial stage. It cannot be neglected that the escaping radicals enter the other monomer-solubilizing micelles (particles) containing oligomer chain(s), of which DP has already attained the  $DP_{cr}$ , resulting in a decrease in the  $N_p$ . In our previous articles, the microemulsion NMP of styrene was carried out at two  $[SG1]_0/[AIBN]_0$  ratios (1.23 and 1.80).<sup>37,55</sup> Similarly in case of the styrene systems, the particle size was larger in the high  $[SG1]_0/[AIBN]_0$  ratio (1.8) than the low one (1.23). In addition,  $N_p$  in the microemulsion NMP of styrene was fixed in the initial stage of the polymerization. Therefore, relationships between the  $[SG1]_0/[AIBN]_0$  ratio and the particle size in both monomers were similar.

Figures 7 and 8 show, respectively, MWDs and  $M_n$  (and  $M_w/M_n$ ) as functions of conversion for the microemulsion NMP with  $[SG1]_0/[AIBN]_0$  (molar ratio) = 1.60, 1.68, 1.76, and 1.92. At the  $[SG1]_0/[AIBN]_0$  ratio of 1.60 (Figures 7a and 8a), the



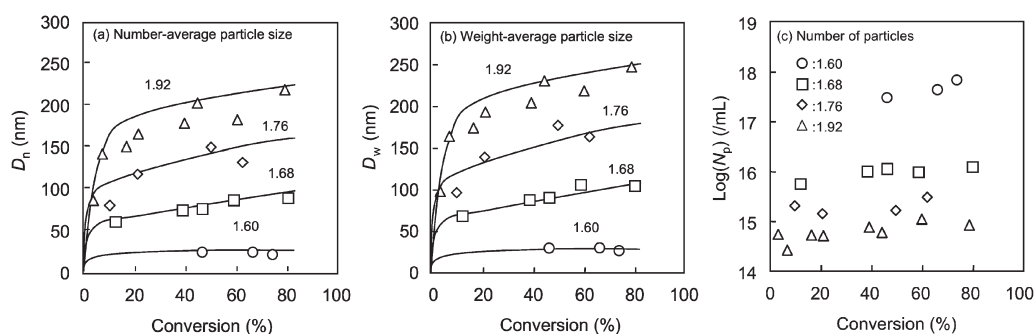


**Figure 5.** (a)  $D_n$ , (b)  $D_w$ , and (c)  $N_p$  versus conversion for microemulsion NMPs of BA using SG1 at 100 °C:  $[AIBN]_0 = 18.6$  mmol/L-monomer;  $[SG1]_0/[AIBN]_0$  (molar ratio) = 1.60 (circles); 1.68 (squares); 1.76 (diamonds); 1.92 (triangles). The lines are guides to the eye only.

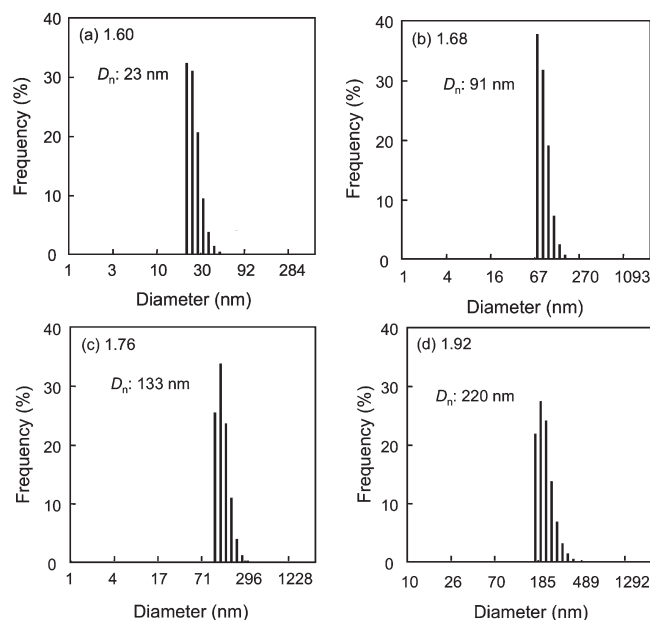


**Figure 6.** Particle size distributions (number distribution) for microemulsion NMPs of BA using SG1 at 100 °C:  $[AIBN]_0 = 18.6$  mmol/L-monomer;  $[SG1]_0/[AIBN]_0$  (molar ratio) = (a) 1.60; (b) 1.68; (c) 1.76; (d) 1.92. Conversions (%): (a) 74; (b) 59; (c) 62; (c) 79.

MWDs were very broad and did not shift to a higher molecular weight with increasing conversion. The values of  $M_n$  decreased with increasing conversion (from 120 000 to 27 000) and the  $M_w/M_n$  values were very high (4.5–8.1), clearly indicating that control/livingness was not obtained. However, at  $[SG1]_0/[AIBN]_0$  ratios of 1.68 (Figure 7b), 1.76 (Figure 7c), and 1.92 (Figure 7d), the MWDs did shift to higher molecular weight with increasing conversion, although in all cases the small tailing at the low molecular weight side was observed, which seem to be caused by the termination reaction during the polymerization.  $M_n$  increased linearly with conversion (Figure 8b) and the  $M_w/M_n$  values were much lower (1.5–2.0) (Figure 8c). In the corresponding homogeneous bulk system, such a character of controlled/living manner was not observed at these  $[SG1]_0/[AIBN]_0$  ratios. These results are consistent with the confined space effect operating on the deactivation reaction in the microemulsion systems, leading to better control over the MWD as well as a reduction in  $R_p$ .

In the microemulsion NMPs, it was found that a relatively small change in  $[SG1]_0/[AIBN]_0$  ratios from 1.60 to 1.68 had a

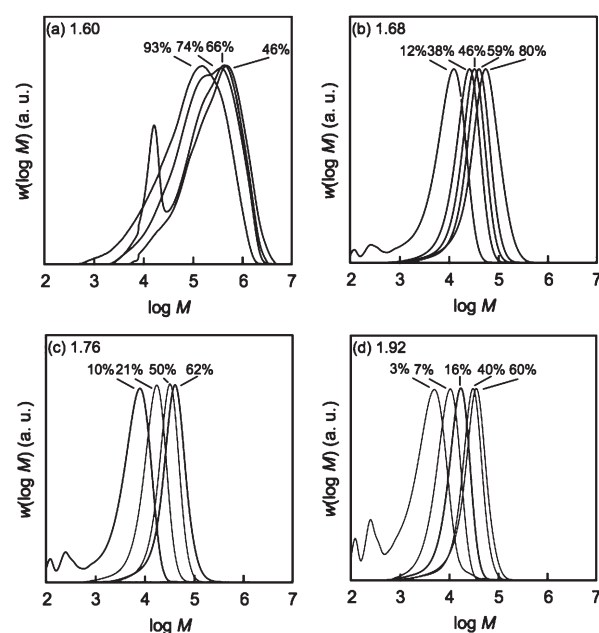


**Figure 7.** MWDs at various conversions for microemulsion NMPs of BA using SG1 at 100 °C:  $[AIBN]_0 = 18.6$  mmol/L-monomer;  $[SG1]_0/[AIBN]_0$  (molar ratio) = (a) 1.60, (b) 1.68, (c) 1.76, and (d) 1.92.

dramatic effect on both  $R_p$  and MWD. In general, in CLRP in aqueous dispersed systems it is important to consider the partitioning of control agent between monomer and aqueous phases. For example, in ATRP system, 90%  $CuBr_2$  (control agent) partitioned to the aqueous phase, resulting in the difficulty of MWD control.<sup>56</sup> However, because only 1% of TEMPO in NMP system partitioned to the aqueous phase<sup>57</sup> and the partition of SG1 seems to be at a similar level,<sup>58</sup> it must be not important for MWD control in microemulsion NMP with SG1. Depending on the value of  $f$ , there exist a critical ratio of  $[SG1]_0/[AIBN]_0$  that gives perfect stoichiometric balance (1:1) between the total number of radicals generated from AIBN and the total number of SG1 radicals. Any change in  $[SG1]_0/[AIBN]_0$  that leads to crossing of this critical ratio will have a very strong effect on the polymerization. The value of  $f$  in the present system is not known with accuracy. However, assuming that the NMPs in Figure 8b proceed according to the ideal NMP mechanism with regards to the number of polymer chains,  $f$  can be estimated to be close to 0.57. However, it has

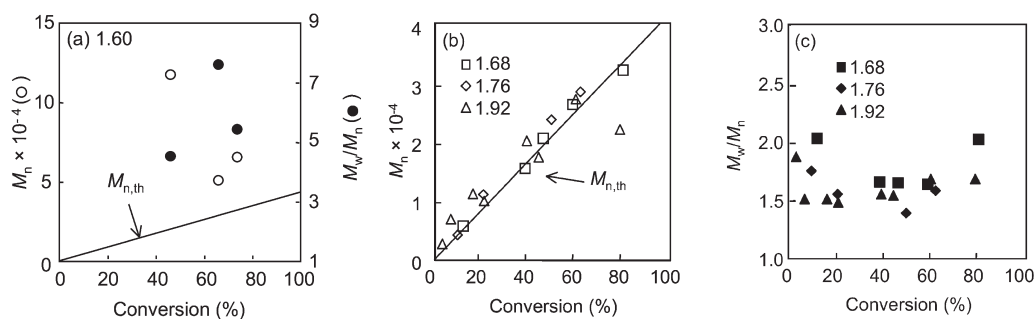


**Figure 8.** (a)  $M_n$  (open circles) and  $M_w/M_n$  (closed circles), (b)  $M_n$ , and (c)  $M_w/M_n$  vs conversion for microemulsion NMPs of BA using SG1 at 100°C:  $[AIBN]_0 = 18.6$  mmol/L-monomer;  $[SG1]_0/[AIBN]_0$  (molar ratio) = 1.60 (circles), 1.68 (squares), 1.76 (diamonds), and 1.92 (triangles).

previously been shown<sup>38</sup> that  $f$  can be somewhat lower in microemulsion systems than homogeneous systems due to geminate termination of initiator radicals, i.e. the confined space effect acting on the initiator radicals generated in pairs. The excess SG1 required to achieve controlled/living character in microemulsion is clearly much lower than for the corresponding bulk system, consistent with the confined space effect operating in the microemulsion system. It is believed that the confined space effect operates in two distinct ways in the present case: (i) It increases the rate of deactivation, and (ii) it increases the rate of geminate termination of initiator radicals. The latter effect also has a beneficial influence on the control over the polymerization, since a lower  $f$  leads to a greater excess of SG1.

## CONCLUSIONS

Microemulsion NMP of BA has been carried out using cationic emulsifier TTAB and nitroxide SG1 at 100°C. At a  $[SG1]_0/[AIBN]_0$  ratio of 1.68, the polymerization rate was low, MWD shifted to higher molecular weight with increasing conversion, and  $M_n$  increased linearly with the conversion close to  $M_{n,th}$  consistent with a controlled/living process, although, the MWD was relatively broad with  $M_w/M_n = 1.5$ –2 throughout the polymerization. In the corresponding bulk NMP, the polymerization rate was extremely high and the MWD revealed no signs of control/livingness. From these results, it is concluded that the superior performance of the microemulsion NMP is caused by the confined space effect: (i) increasing the rate of deactivation and (ii) increasing the rate of geminate termination of initiator radicals (leading to a greater excess of SG1). In a following paper, we will discuss the confined space effect especially in the initial stage of the microemulsion NMP of BA, in which the size of monomer-solubilizing micelles was approximately 2 nm, in comparison with miniemulsion NMP (droplet/particle size was approximately 60 nm throughout the polymerization). The chain extension test of PBA obtained in the initial stages of the microemulsion and miniemulsion NMPs will also be attempted in bulk NMP of styrene.

## AUTHOR INFORMATION

### Corresponding Author

\*E-mail: okubo@kobe-u.ac.jp.

### Notes

<sup>†</sup>Part CCCXLIII of the series “Studies on Suspension and Emulsion”.

### Present Addresses

<sup>‡</sup>Centre of Advanced Macromolecular Design (CAMD), School of Chemical Science and Engineering, The University of New

South Wales, Sydney, NSW 2052, Australia. Telephone: +61-2-9385-4331. Fax: +61-2-9385-6250

## ACKNOWLEDGMENT

This work was partially supported by a Grant-in-Aid for Scientific Research (A) (Grant 21245050) from the Japan Society for the Promotion of Science (JSPS), and Kobe University Takuetsu-shita Research Project grant. We appreciate to ARKEMA K.K. for donating the nitroxide SG1.

## REFERENCES

- Braunecker, W.; Matyjaszewski, K. *Prog. Polym. Sci.* **2007**, *32*, 93–146.
- Georges, M. K.; Veregin, R. P. N.; Kazmaier, P. M.; Hamer, G. K. *Macromolecules* **1993**, *26*, 2987–2988.
- Hawker, C. J.; Bosman, A. W.; Harth, E. *Chem. Rev.* **2001**, *101*, 3661–3688.
- Matyjaszewski, K.; Xia, J. *Chem. Rev.* **2001**, *101*, 2921–2990.
- Kamigaito, M.; Ando, T.; Sawamoto, M. *Chem. Rev.* **2001**, *101*, 3689–3745.
- Moad, G.; Rizzardo, E.; Thang, S. H. *Aust. J. Chem.* **2006**, *59*, 669–692.
- Zetterlund, P. B.; Kagawa, K.; Okubo, M. *Chem. Rev.* **2008**, *108* (9), 3747–3794.
- Cunningham, M. F. *Prog. Polym. Sci.* **2008**, *33* (4), 365–398.
- Kitayama, Y.; Yorizane, M.; Kagawa, Y.; Minami, H.; Zetterlund, P. B.; Okubo, M. *Polymer* **2009**, *50*, 3182–3187.
- Kitayama, Y.; Kagawa, Y.; Minami, H.; Okubo, M. *Langmuir* **2010**, *26*, 7029–7034.
- Tanaka, T.; Okayama, M.; Kitayama, Y.; Kagawa, Y.; Okubo, M. *Langmuir* **2010**, *26*, 7843–7847.
- Tanaka, T.; Okayama, M.; Minami, H.; Okubo, M. *Langmuir* **2010**, *26*, 11732–11736.
- Butte, A.; Storti, G.; Morbidelli, M. *DEHEMA Monogr.* **1998**, *134*, 497–507.
- Charleux, B. *Macromolecules* **2000**, *33*, 5358–5365.
- Zetterlund, P. B.; Okubo, M. *Macromolecules* **2006**, *39*, 8959–8967.
- Kagawa, Y.; Zetterlund, P. B.; Minami, H.; Okubo, M. *Macromol. Theory Simul.* **2006**, *15*, 608–613.
- Tobita, H. *Macromol. Theory Simul.* **2007**, *16*, 810–823.
- Tobita, H.; Yanase, F. *Macromol. Theory Simul.* **2007**, *16*, 476–488.
- Zetterlund, P. B.; Okubo, M. *Macromol. Theory Simul.* **2007**, *16*, 221–226.
- Zetterlund, P. B.; Kagawa, Y.; Okubo, M. *Macromolecules* **2009**, *42* (7), 2488–2496.
- Zetterlund, P. B.; Okubo, M. *Macromol. Theory Simul.* **2009**, *18*, 277–286.

- (22) Zetterlund, P. B. *Macromolecules* **2010**, *43*, 1387–1395.
- (23) Zetterlund, P. B. *Macromol. Theory Simul.* **2010**, *19*, 11–23.
- (24) Thomson, M. E.; Cunningham, M. F. *Macromolecules* **2010**, *43*, 2772–2779.
- (25) Tobita, H. *Macromol. React. Eng.* **2010**, *4*, 643–662.
- (26) Zetterlund, P. B. *Polym. Chem.* **2011**, *2*, 534–549.
- (27) Tobita, H. *Macromol. Theory Simul.* **2011**, *20*, 179–190.
- (28) Guo, J. S.; El-Aasser, M. S.; Vanderhoff, J. W. *Microemulsion Polymerization of Styrene*; El-Nokaly, M. A., Ed.; ACS Symposium Series 384; American Chemical Society: Washington, DC, 1989; pp 86–99.
- (29) Paul, B. K.; Moulik, S. P. *Curr. Sci.* **2001**, *80*, 990.
- (30) Chow, P. Y.; Gan, L. M. *Adv. Polym. Sci.* **2005**, *175*, 257–298.
- (31) Hermanson, K. D.; Liu, S. Y.; Kaler, E. W. *J. Polym. Sci.; Part A: Polym. Chem.* **2006**, *44*, 6055–6070.
- (32) O'Donnell, J.; Kaler, E. W. *Macromolecules* **2008**, *41*, 6094–6099.
- (33) O'Donnell, J.; Kaler, E. W. *Macromolecules* **2010**, *43*, 1730–1738.
- (34) Min, K.; Matyjaszewski, K. *Macromolecules* **2005**, *38*, 8131–8134.
- (35) Min, K.; Gao, H.; Matyjaszewski, K. *J. Am. Chem. Soc.* **2006**, *128*, 10521–10526.
- (36) Kagawa, Y.; Kawasaki, M.; Zetterlund, P. B.; Minami, H.; Okubo, M. *Macromol. Rapid Commun.* **2007**, *28*, 2354–2360.
- (37) Wakamatsu, J.; Kawasaki, M.; Zetterlund, P. B.; Okubo, M. *Macromol. Rapid Commun.* **2007**, *28*, 2346–2353.
- (38) Zetterlund, P. B.; Wakamatsu, J.; Okubo, M. *Macromolecules* **2009**, *42*, 6944–6952.
- (39) Kagawa, Y.; Kawasaki, M.; Zetterlund, P. B.; Minami, H.; Okubo, M. *Macromol. Rapid Commun.* **2007**, *28*, 2354–2360.
- (40) Maehata, H.; Buragina, C.; Cunningham, M. F. *Macromolecules* **2007**, *40*, 7126–7131.
- (41) Asua, J. M.; Beuermann, S.; Buback, M.; Castignolles, P.; Charleux, B.; Gilbert, R. G.; Hutchinson, R. A.; Leiza, J. R.; Nikitin, A. N.; Vairon, J. P.; van Herk, A. M. *Macromol. Chem. Phys.* **2004**, *205* (16), 2151–2160.
- (42) Studer, A.; Harms, K.; Knoop, C.; Muller, C.; Schulte, T. *Macromolecules* **2004**, *37*, 27–34.
- (43) Knoop, C. A.; Studer, A. *J. Am. Chem. Soc.* **2003**, *125*, 16327–16333.
- (44) Wetter, C.; Gierlich, J.; Knoop, C. A.; Muller, C.; Schulte, T.; Studer, A. *Chem.—Eur. J.* **2004**, *10*, 1156–1166.
- (45) Benoit, D.; Grimaldi, S.; Finet, J. P.; Tordo, P.; Fontanille, M.; Gnanou, Y. *Controlled/Living Free-Radical Polymerization of Styrene and n-Butyl Acrylate in the Presence of a Novel Asymmetric Nitroxyl Radical*; American Chemical Society: Washington, DC, 1998; p 225.
- (46) Benoit, D.; Chaplinski, V.; Braslau, R.; Hawker, C. J. *J. Am. Chem. Soc.* **1999**, *121*, 3904–3920.
- (47) Benoit, D.; Grimaldi, S.; Robin, S.; Finet, J.-P.; Tordo, P.; Gnanou, Y. *J. Am. Chem. Soc.* **2000**, *122*, 5929–5939.
- (48) Lacroix-Desmazes, P.; Lutz, J.-F.; Chauvin, F.; Severac, R.; Boutevin, B. *Macromolecules* **2001**, *34*, 8866–8871.
- (49) Chauvin, F.; Dufils, P. E.; Gigmes, D.; Guillauneuf, Y.; Marque, S. R. A.; Tordo, P.; Bertin, D. *Macromolecules* **2006**, *39*, 5238–5250.
- (50) Gigmes, D.; Bertin, D.; Lefay, C.; Guillauneuf, Y. *Macromol. Theory Simul.* **2009**, *18*, 402–419.
- (51) Buback, M.; Huckestein, B.; Kuchta, F.-D.; T., R. G.; Schmid, E. *Macromol. Chem. Phys.* **1994**, *195*, 2117–2140.
- (52) Luo, Y.; Tsavalas, J.; Schork, F. J. *Macromolecules* **2001**, *34*, 5501–5507.
- (53) Ugelstad, J.; Kaggerud, K. H.; Hansen, F. K.; Berge, A. *Makromol. Chem.* **1979**, *180*, 737–744.
- (54) Ugelstad, J.; Mork, P. C.; Kaggerud, K. H.; Ellingsen, T.; Berge, A. *Adv. Colloid Interface Sci.* **1980**, *13*, 101–140.
- (55) Zetterlund, P. B.; Wakamatsu, J.; Okubo, M. *Macromolecules* **2009**, *42*, 6944–6952.
- (56) Kagawa, Y.; Zetterlund, P. B.; Minami, H.; Okubo, M. *Macromolecules* **2007**, *40*, 3062–3069.
- (57) Ma, J. W.; Cunningham, M. F.; McAuley, K. B.; Keoshkerian, B.; Georges, M. K. *J. Polym. Sci.; Part A: Polym. Chem.* **2001**, *39*, 1081–1089.
- (58) Delaître, G.; Charleux, B. *Macromolecules* **2008**, *41*, 2361–2367.